Original Article

Correlation analysis of organ doses with dose metrics for patients undergoing organ dose-modulated head CT examinations

Mengting Wang[1,2#], Tian Qin[1#], Yihan Fan[1], Zongyu Xie[3], Baohui Liang[1]

[1]School of Medical Imaging, Bengbu Medical University, Bengbu, China; [2]Department of Oncology, the Second Hospital of Anhui Medical University, Hefei, China; [3]Department of Radiology, the First Affiliated Hospital of Bengbu Medical University, Bengbu, China

Contributions: (I) Conception and design: B Liang, M Wang; (II) Administrative support: B Liang; (III) Provision of study materials or patients: T Qin, M Wang; (IV) Collection and assembly of data: M Wang, T Qin; (V) Data analysis and interpretation: M Wang, T Qin, Y Fan; (VI) Manuscript writing: All authors; (VII) Final approval of manuscript: All authors.

[#]These authors contributed equally to this work.

Correspondence to: Baohui Liang, PhD. School of Medical Imaging, Bengbu Medical University, 2600 Donghai Road, Bengbu 233030, China. Email: yxwlx@126.com.

Background: The rapid advancement of computed tomography (CT) has greatly improved clinical diagnosis but has also introduced new challenges in radiation protection. This study aimed to evaluate the relationship between organ doses from Monte Carlo (MC) simulations and CT dose metrics for head CT exams with organ dose modulation (ODM), and to develop a simplified method for estimating individual organ doses.

Methods: A CT source model including the X-ray energy spectrum, bowtie filter, fan beam shape, and rotational motion of the tube was constructed and validated. The modeling was divided into two different exposure regions based on the ODM technical principles: the 100° range on the anterior side of the skull (tube current reduction region) and the remaining 260° (tube current constant region). The source model was validated by comparing the error between the MC-simulated weighted CT dose index ($CTDI_w$) and the measured $CTDI_w$. A total of 40 patients were retrospectively collected, and each patient's voxelized head models were constructed and used for MC simulation to calculate organ doses. The global volume CTDI ($CTDI_{vol}$), regional $CTDI_{vol}$, size-specific dose estimate (SSDE), and organ-specific SSDE were derived based on the exposure (mAs) and water-equivalent diameters of each slice image. Linear regression fitting was used to explore the correlation between organ doses (including the brain, the eyeballs, the eye lens, and the salivary glands) and the four CT dose metrics mentioned above.

Results: Comparison results for $CTDI_w$ showed that the simulated source model error was within 5%, and the ODM model's error was below 0.05%. Organ doses correlated strongly with organ-specific SSDE (The R^2 between each organ dose and corresponding organ-specific SSDE were 0.92 for the brain, 0.91 for eyeballs, 0.90 for the eye lens, and 0.90 for the salivary gland). Estimation coefficients for estimating organ doses of the brain, eyeballs, eye lens, and salivary glands from organ-specific SSDE were 0.34, 0.59, 0.48, and 0.26, respectively, as a mean across all patients.

Conclusions: There is a strong correlation between organ dose and organ-specific SSDE in ODM head CT examinations. However, activating the ODM results in significant differences in estimation coefficients for head CT exams with a fixed tube current, which provides a practical way to determine organ doses for individual patients undergoing head CT scans.

Keywords: Computed tomography (CT); Monte Carlo (MC); organ dose modulation (ODM); size-specific dose estimate (SSDE)

Submitted Sep 25, 2024. Accepted for publication Mar 11, 2025. Published online Apr 28, 2025.
doi: 10.21037/qims-24-2061
View this article at: https://dx.doi.org/10.21037/qims-24-2061

Introduction

Computed tomography (CT) is widely used as the first choice of imaging modality for the head, hypopharynx, sinus area, and temporal bone (1). However, it is essential to be aware that overexposure of the lens of the eye during a head CT examination can result in radiation damage, including cataracts, blurry vision, and clouding of the eyeball (2,3). A team of researchers further found that the incidence of benign and malignant tumors of the brain increased dose-dependently with the frequency of head CT examinations in children and young adults (4,5). Adhering to the as low as reasonably achievable (ALARA) principle emphasizes the importance of minimizing radiation dose during a CT examination while ensuring that image quality remains uncompromised, which is also suitable for head CT examinations. Due to the high sensitivity of superficial organs in the anterior of the skull to X-rays, organ dose modulation (ODM) is an effective technique that enables lower tube current when the tube moves to the anterior of the patient's body or head, thus reducing radiation dose to sensitive organs such as the lens. This method also presents great potential for achieving targeted protection of superficial organs while maintaining overall image quality (6-8).

During CT examinations, the implementation of ODM technology has posed new challenges for accurately estimating organ dose. Although Monte Carlo (MC) simulation is the most precise method for calculating individualized organ dose, it can also be time-consuming and labor-intensive (9). In recent years, researchers have developed the MC model based on graphic processing unit (GPU) acceleration, which greatly improves the computational efficiency, but this requires a certain level of performance from the computer being used (10). Since the exact algorithms for ODM are often unknown, very little work has been done to explore organ dose in ODM. As a result, there is a rising demand for a quick and reliable method of acquiring organ dose during ODM CT examinations. Numerous studies have revealed a correlation between the organ dose derived from MC simulation and alternative dose metrics. This link may be utilized to quickly approximate organ dose in patients who have undergone ODM CT examinations (11-16). Hardy *et al.* discovered that the size-specific dose estimate (SSDE) had a high correlation with organ doses in thoracic abdomen pelvic CT examination (14). According to a study conducted by Fujii *et al.*, there is a significant correlation between the organ dose estimated through MC simulation and organ-specific SSDE in patients undergoing chest-abdomen-pelvis CT examinations (16). Many studies have mainly focused on determining organ dose in CT examinations through fixed-tube current or Z-axis tube current modulation, raising concerns about organ dose estimation with ODM technology. This work aimed to develop a more accurate and efficient method of determining the individualized estimation of organ doses for patients undergoing head CT examinations with ODM with Revolution CT scanner from General Electric (GE) manufacturers (Chicago, IL, USA), which was installed in the First Affiliated Hospital of Bengbu Medical University in Bengbu, China. We present this article in accordance with the STROBE reporting checklist (available at https://qims.amegroups.com/article/view/10.21037/qims-24-2061/rc).

Methods

Patient data collection

A retrospective study was carried out on a cohort of 40 patients who underwent head CT examinations utilizing ODM between June 2023 and August 2023 at the First Affiliated Hospital of Bengbu Medical University. The examinations were performed on Revolution CT scanner (GE Healthcare), where the ODM technology was enabled. A specific description of the ODM technique is provided in the *Methods* section, second paragraph of the CT scanner modeling section.

This study was performed with the approval of Bengbu Medical University Ethics Committee (No. 2021-292) and was conducted following the guidelines of the Declaration of Helsinki (as revised in 2013). The Ethics Committee waived the need for informed consent for this retrospective study.

Construction of patient models

Quantifying the radiation dose delivered to various organs of patients is crucial for ensuring radiation protection.

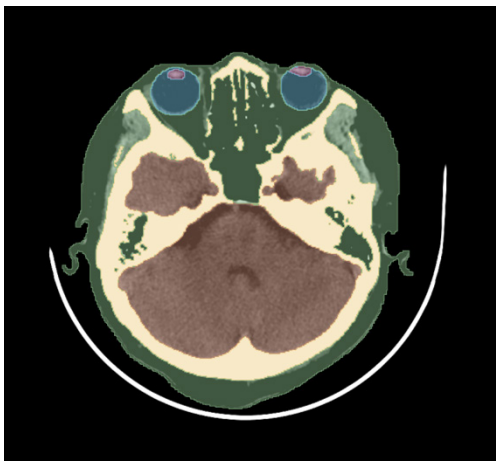

Figure 1 Schematic drawing of the organ using 3D Slicer software.

However, direct measurement of organ doses using dosimeters is both complex and challenging, but more importantly, impossible for patients undergoing CT examinations. In this regard, MC simulations have become the first choice for accurate assessment of organ doses. A total of 40 patients were included in this study, and digital voxel models were created for each patient using a series of steps: the slice images were imported into the 3D Slicer software (https://www.slicer.org/), and the skull was outlined by setting the Hounsfield unit (HU) value threshold range, whereas the brain was outlined using automatic contouring. The lens, eyeballs, and salivary glands were segmented manually. After segmentation, the segmentation information was saved in Digital Imaging and Communications in Medicine for Radiation Therapy (DICOM-RT) format and imported into our GUI program written in MATLAB (https://www.mathworks.com/products/matlab.html) for voxelization. The elemental composition and physical density of each organ in the head voxelized model were defined based on the information in the International Commission on Radiological Protection (ICRP) Publication 110 (*Figure 1*).

CT scanner modeling

Our CT source model and bowtie filter were constructed using the methods developed by Turner *et al.*, including the generation of equivalent energy spectra by the half-value layer (HVL) method and the construction of bowtie filters by the error of weighted CT dose index ($CTDI_w$) (17). The specific details are as follows: a pencil ionization chamber and aluminum sheets of different thicknesses were initially employed to measure the HVL_1 with various tube voltages. We then aligned the obtained HVL_1 values with the HVL output from SPEKTR 3.0 spectroscopy software (18), resulting in an equivalent energy spectrum at the designated tube voltage. In this study, the intricate structure of the bowtie filter presented difficulty in developing a precise model due to the manufacturer's lack of specific geometric details. We created a simplified version to address this issue by utilizing a rectangular body with an ellipsoid removed. The usability of the constructed bowtie filter model was validated by making the $CTDI_w$ obtained from the simulation have a small error with respect to the $CTDI_w$ measured in the field by adjusting the radius of the long and short axis of the ellipse and the depth of its embedding in the rectangle. The bowtie filter's material was aluminum; according to the procedures outlined by Gu and Pan *et al.* to generate a sector-shaped X-ray beam (19,20), the internal cookie-cutter function of the Monte Carlo N-Particle (MCNP) software was used as a generic source model for Revolution CT to define the orientation and collimation of the X-ray beam.

Based on the concept of "dose equivalence", a certain number of X-ray sources are set up within a certain distance from the isocenter to simulate a CT single-slice axial scan. In our parameter settings, this value was set to 62.56 cm (corresponding to the source's distance from the isocenter in the Revolution CT user manual). It is worth noting that the more X-ray sources used in the simulation, the more accurate the results will be. However, an increase in the number of sources is also associated with a much longer simulation time, driving a need to strike a balance between the number of sources and the accuracy of the simulation. Gu *et al.* found that the errors between the simulated values of $CTDI_{100}$ and the actual measurements were within 5% for 24 and 32 sources during one X-ray tube rotation (19). Therefore, we finally determined to set up 32 sources around the patient. According to the Revolution CT user manual, the ODM lowers the tube current in the ±50° range with 0 degrees at the anterior region of the skull, while leaving the tube current in the other angles unchanged in one rotation (*Figure 2A*), thus allowing dose reduction of many sensitive organs in the anterior part of the head and body. During the MC simulation, emitting two X-ray energies simultaneously is quite challenging. Given that the two different energies of the X-ray source utilized in the ODM technique operate under the same tube voltage while exhibiting different tube currents, we partitioned

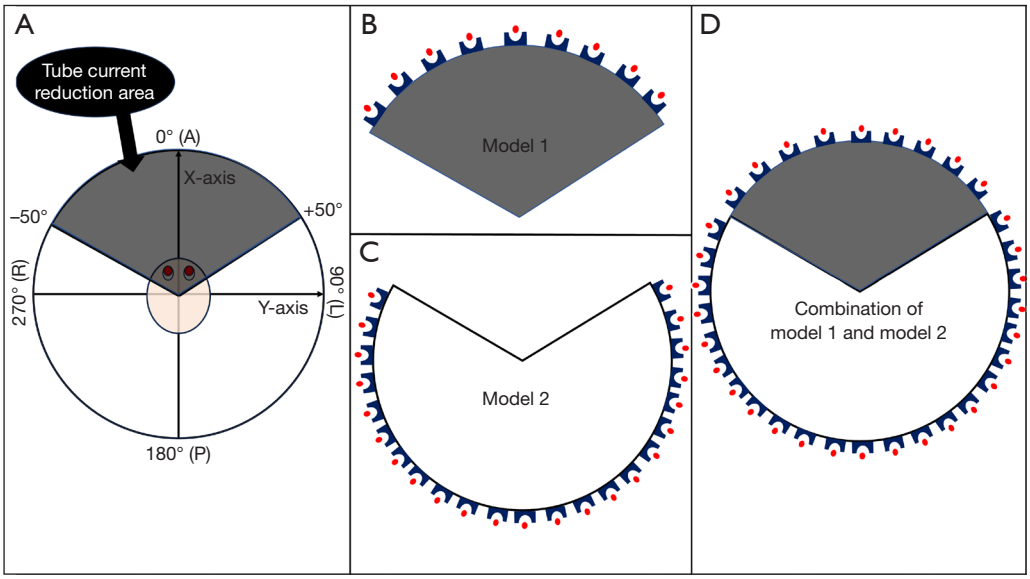

Figure 2 Schematic and modeling diagram of Revolution CT's ODM technology. (A) Modulation of ODM technology. (B) Illustration of 9 X-ray sources in the anterior region of a head CT scan for simulating the output of the exposure in the ODM range. (C) Model 2: Illustration of 23 X-ray sources within 260° and bowtie filters for simulating the exposure output without the ODM technique. (D) The combined output of model 1 and model 2 represents a 360° source. A, anterior; CT, computed tomography; L, left; ODM, organ dose modulation; P, posterior; R, right.

the 360° distributed source into two segments for the MC simulation. Each segment was designated an individual exposure level, Model 1 (9 sources and 9 bowtie filters) for the 100° and Model 2 (23 sources and 23 bowtie filters) for the 260° (*Figure 2B,2C*). The results of these simulations were subsequently aggregated to formulate what is referred to as the equivalent 360° source model, which serves to approximate the actual 360° CT scan (*Figure 2D*). Based on the above principles, two individual scans of the same slice are required.

Validation of CT scanner models

For the X-ray energies used in CT scanners, when a photon comes into contact with an object, electrons resulting from the photoelectric effect and Compton scattering are assumed to travel in the direction of the primary photon, and electron energy is deposited at the location where they interact with the photon to satisfy the charged-particle equilibrium (CPE) condition (21). Under this circumstance, the collision-specific kinetic energy is approximately equal to the absorbed dose of the organ, so the F6 card, which is used to count the collision kerma, was chosen in this study to record the energy deposition results. The F6 card normalizes the simulation results to individual particles in Mev/gram/particle units. The conversion of the units is carried out utilizing a conversion factor (CF), which is calculated as follows:

$$CF = \frac{CTDI_{100,M}}{CTDI_{100,S}} \quad [1]$$

where $CTDI_{100,M}$ is the $CTDI_{100}$ value in mGy/100mAs for air at the isocenter of the CT gantry measured *in situ* in a pencil ionization chamber (RaySafe Xi; RaySafe AB Corporation, Billdal, Sweden) and $CTDI_{100,S}$ is the simulated MC value in MeV/gram/particle for the same scan protocol within a same simulation pencil ionization chamber. The pencil ionization chamber parameters used for the modeling were obtained from the manufacturers (*Figure 3*).

To verify the accuracy of the CT source model, we have compared experimental measurements with MC simulations. The dose values of the CTDI phantom were measured using the pencil ionization chamber, which was inserted into each of the five holes of the phantom for experimental measurement. The remaining holes were plugged with polymethylmethacrylate (PMMA) sticks, except for that filled by the ionization chamber, to obtain the $CTDI_W$

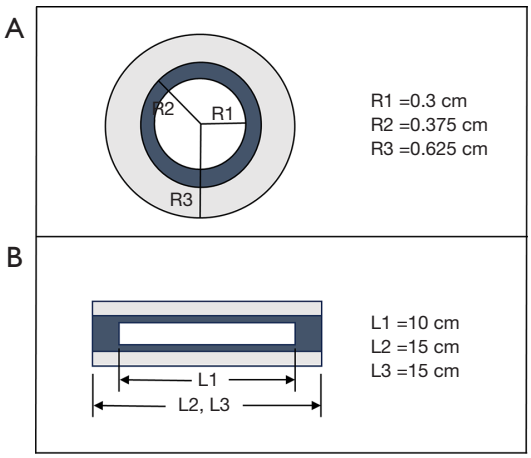

Figure 3 Geometry and material composition of the pencil ionization chamber. L, length; R, radius.

values. For MC simulations, a CTDI phantom with a diameter of 16 cm and a length of 15 cm was constructed along with the pencil ionization chamber. Simulations were performed to compute the $CTDI_{100}$ values for the centers and edges of the CTDI phantom, following a process similar to that of the experimental measurement.

Validation of ODM technique models

It is worth noting that in verifying the feasibility of performing a 360° scan in two parts, we verified this separate simulation in the normal scan mode (same exposure) because it was not possible to simulate both exposures similarly to the ODM in MCNP in one rotation. We used MCNP simulations to verify the error between the air $CTDI_{100}$ at the isocenter for 360° scans in normal scanning mode (non-ODM mode) and the sum of air $CTDI_{100}$ at the isocenter for 100° (Model 1) and 260° (Model 2) scans. Analysis was thereby conducted regardless of whether the exposures has been simulated separately, according to the angular range affects the final results.

Radiation dose metrics for head CT examinations

Calculation of dose metrics

$CTDI_{vol}$, as an important dose metric in CT examination, has two notable limitations: first, with the application of tube current modulation, it can only reflect the average radiation dose over the entire scanning range, and is thus unable to exhibit the difference of various organs. Based on this limitation, Khatonabadi *et al.* proposed the concept of regional $CTDI_{vol}$, which represents the $CTDI_{vol}$ at the range where the studied organ is located (22). Second, $CTDI_{vol}$ merely indicates the dose output by the CT scanner to the standard CTDI dose phantom and lacks consideration of differences in the body size of those being analyzed. To address this concern, the American Association of Physicists in Medicine (AAPM) Report 204 proposed SSDE based on effective diameter, followed by improved concepts in Reports 220 and 293 called SSDE based on water equivalent diameter (WED) and organ-specific SSDE (23,24). Both of these metrics are patient-specific and effectively tackle the challenges of dose characterization for patients with differing body sizes. In our study, four radiation dose metrics were involved: dose-reported global $CTDI_{vol}$, organ-based regional $CTDI_{vol}$, SSDE based on global $CTDI_{vol}$, and organ-specific SSDE.

Calculation of the regional $CTDI_{vol}$ for each organ first requires obtaining the tube current modulation profile for each patient. The organ-based regional $CTDI_{vol}$ can be calculated based on the relationship between the average tube current applied to the specific organ and the average tube current used throughout the global scan range. The calculation method is shown in Eq. [2].

$$Regional\ CTDI_{vol} = \frac{Global\ CTDI_{vol}}{I_i} \times \frac{\sum_n^{n+k} i}{k} \quad [2]$$

where I_i represents the mean tube current over all scan range, i represents the tube current in the organ, n represents the first slice of the organ, and k is the number of slices occupied by the organ.

All slice images of 40 patients were imported using ImageJ software (National Institutes of Health, Bethesda, MD, USA) and the region of interest (ROI) was outlined. A method for calculating the SSDE based on the WED was presented in AAPM Report 293. Taking a single patient as an example: after loading all the slice images, the external contour of the patient was outlined as the ROI using ImageJ's built-in threshold segmentation function; the area of the ROI and the mean of the HU values were measured and recorded. Subsequently, the WED was calculated according to Eq. [3], and based on the WED, the body size correction factor f^{H16} and the SSDE were derived using Eqs. [4,5]. The equations are as follows:

$$WED = 2\sqrt{\left[\frac{1}{1000} HU\left(x,y\right)_{ROI} + 1\right]\frac{A_{ROI}}{\pi}} \quad [3]$$

$$f^{H16} = \alpha \times e^{-\beta * WED} \quad [4]$$

$$SSDE = f^{H16} \times Global\ CTDI_{vol} \quad [5]$$

where $HU\ (x, y)_{ROI}$ is the average HU value in the ROI, A_{ROI} is the area of ROI. Of the constants given in Report 293: α=1.9852, β=0.486.

Organ-specific WED was defined as the average WED of the slice images corresponding to the z-axis position of each organ. We obtained the organ-specific SSDE by multiplying the organ-based regional $CTDI_{vol}$ of each organ by f_{organ}^{H16} derived from the organ-specific WED. The equations used are as follows:

$$WED_{organ} = \frac{1}{k}\sum_{n}^{n+k}\sqrt[2]{\left[\frac{1}{1000}HU\left(x,y\right)_{ROI}+1\right]\frac{A_{ROI}}{\pi}} \quad [6]$$

$$SSDE_{organ} = CTDI_{vol} \times f_{organ}^{H16} \quad [7]$$

where $HU\ (x, y)_{ROI}$ denotes the average HU value in the ROI delineating the patient's body contour in each slice, A_{ROI} denotes the area of this ROI, and f_{organ}^{H16} is the average of the f^{H16} at all slices where the organ is located.

Calculation of organ dose for each patient

The constructed CT source models of 100° and 260° moving along the Z-axis direction of the voxelized head model were used to simulate ODM scanning. The results were recorded, accumulated, and summed as the total dose for each organ. The GE Revolution CT user manual shows that the ODM technique reduces the tube current in the anterolateral 100° range by 30% in head CT examinations. In contrast, the tube current in the remaining angles remains the same as when the ODM technique is not enabled. Based on the modulation principle of the ODM technique, the exposure (mAs) were calculated for the modulated and non-modulated angular ranges of tube current, respectively.

In order to determine the organ dose per slice within each angular range, the simulation results' units must be converted from MeV/gram/particle to mGy/100 mAs using the CF, as described in the section of *Validation of CT scanner models*. Given that the F6 card normalizes the results to individual particles, the equations for this calculation are provided below:

$$D_{Ti1} = D_{s1} \times CF \quad [8]$$

$$D_{Ti2} = D_{s2} \times CF \quad [9]$$

D_{S1} is the result of the MC simulation of each organ at each slice of scanning for the 100° model, and D_{S2} is the result of the MC simulation of each organ at each scanning slice for the 260° model.

D_{Ti1} and D_{Ti2} were multiplied by the mAs of the corresponding angular range in each slice, and the results of the two parts were added up to be the radiation dose of each organ in that slice; finally, the dose of each slice in the scanning range was added slice by slice to obtain the organ dose of each organ. The equation is as follows:

$$D_T = \sum_{i=1}^{k}\left[D_{Ti1} \times \frac{I_{i1}}{100} + D_{Ti2} \times \frac{I_{i2}}{100}\right] \quad [10]$$

in this equation, I_{i1} is the mAs in the 100° per slice range, I_{i2} is the mAs value in the 260° per slice range, and k is the number of slices occupied by the organ.

Statistical analysis

Correlations between organ dose and four dose metrics ($CTDI_{vol}$, organ-specific $CTDI_{vol}$, SSDE, and organ-specific SSDE) were assessed by linear regression fitting using Origin software version 2022 (OriginLab Corp., Northampton, MA, USA). The determination coefficient, R^2, was also considered an important parameter to assess the degree of correlation between the two-dose metrics, with higher values of R^2 indicating a higher degree of linear correlation between the two variables.

Results

Validation of ODM technique models

Table 1 shows the results of $CTDI_{100}$ of the air at the isocenter for the three source models in MC simulation (100°, 260°, 360°). The results show that the error between the $CTDI_{100}$ of the 360° source model and the cumulative $CTDI_{100}$ of the Model 1 (100°) and Model 2 (260°) source models is less than 0.05% for both collimations at all tube voltages.

CF for head CT examinations

In order to verify the CT source model and compute organ dose values from head CT scan, we used a CF responsible for translating the MeV/gram/particle from the MC simulation outcomes to mGy/100 mAs. The CF differs according to the scanning protocol employed, as

Table 1 Comparison of $CTDI_{100}$ of the air at the isocenter for the sum of two CT source models and for 360° scanning

kV	Collimation (mm)	100° (Model 1) $CTDI_{100}$	260° (Model 2) $CTDI_{100}$	Sum	360° model $CTDI_{100}$	Error (%)
80	40	2.769E–09	1.233E–05	1.234E–05	1.234E–05	0.036
	80	1.295E–09	8.894E–06	8.895E–06	8.894E–06	–0.016
100	40	2.506E–09	1.275E–05	1.275E–05	1.274E–05	–0.037
	80	1.293E–09	8.484E–06	8.485E–06	8.489E–06	0.050
120	40	2.028E–09	1.317E–05	1.317E–05	1.317E–05	–0.009
	80	1.039E–09	8.356E–06	8.357E–06	8.358E–06	0.015
140	40	2.140E–09	1.369E–05	1.369E–05	1.369E–05	–0.008
	80	9.634E–10	8.339E–06	8.393E–06	8.390E–06	–0.038

CT, computed tomography; $CTDI_{100}$, CT dose index 100.

Table 2 Dose conversion factors in head examinations

kV	Collimation (mm)	$CTDI_{100}$ measured in air (mGy/100 mAs)	$CTDI_{100}$ simulated in air (MeV/gram/particle)	CF (mGy•gram•particle/100 mAs/MeV)
80	40	9.756	1.289E–05	7.567E+05
	80	8.876	6.447E–06	1.377E+06
100	40	16.200	1.311E–05	1.235E+06
	80	14.730	6.557E–06	2.246E+06
120	40	23.625	1.349E–05	1.752E+06
	80	21.514	6.743E–06	3.191E+06
140	40	32.050	1.414E–05	2.267E+06
	80	29.225	7.069E–05	4.134E+06

CF, conversion factor; CT, computed tomography; $CTDI_{100}$, CT dose index 100.

shown in *Table 2*.

Validation of CT source models

The $CTDI_w$ of in-field measurements and MC simulations with various scanning protocols were calculated. The results of the comparison are shown in *Table 3*. Notably, the measured and simulated values differ within 5%.

Organ dose for head CT scan with ODM technology

The correlations of organ doses for 40 individual patients with the global $CTDI_{vol}$, organ-based regional $CTDI_{vol}$, SSDE, and organ-specific SSDE were evaluated separately using linear regression fitting, and estimation coefficients (i.e., the slope) for estimating organ doses based on each dose metric were derived (for an example, see *Figure 4*). The linear correlation between organ dose and organ-specific SSDE ($R^2 \geq 0.90$) was more robust than the linear correlations between organ dose and the other dose value metrics: global $CTDI_{vol}$ ($R^2 \geq 0.42$), organ-based regional $CTDI_{vol}$ ($R^2 \geq 0.52$), and SSDE ($R^2 \geq 0.73$). Based on derived linear regression equations, the estimation coefficients using organ-specific SSDE to assess the organ dose for the four studied organs (brain, eyeballs, lens, and salivary glands) were 0.34, 0.59, 0.48, and 0.26, respectively.

Discussion

This study involved creating two CT source models with varying mAs magnitudes for organ dose calculation, utilizing the ODM technique's tube current modulation range,

Table 3 Measured versus simulated $CTDI_w$ values for different scanning protocols for head CT examinations

kV	Collimation (mm)	$CTDI_w$ measured (mGy/100 mAs)	$CTDI_w$ simulated (mGy/100 mAs)	Error (%)
80	40	6.170	5.984	3.113
	80	5.452	5.444	0.134
100	40	10.804	10.981	−1.615
	80	9.542	9.984	−4.428
120	40	16.527	16.896	−2.183
	80	14.768	15.386	−4.022
140	40	22.904	23.557	−2.770
	80	20.875	21.480	−2.817

CT, computed tomography; $CTDI_w$, weighted CT dose index.

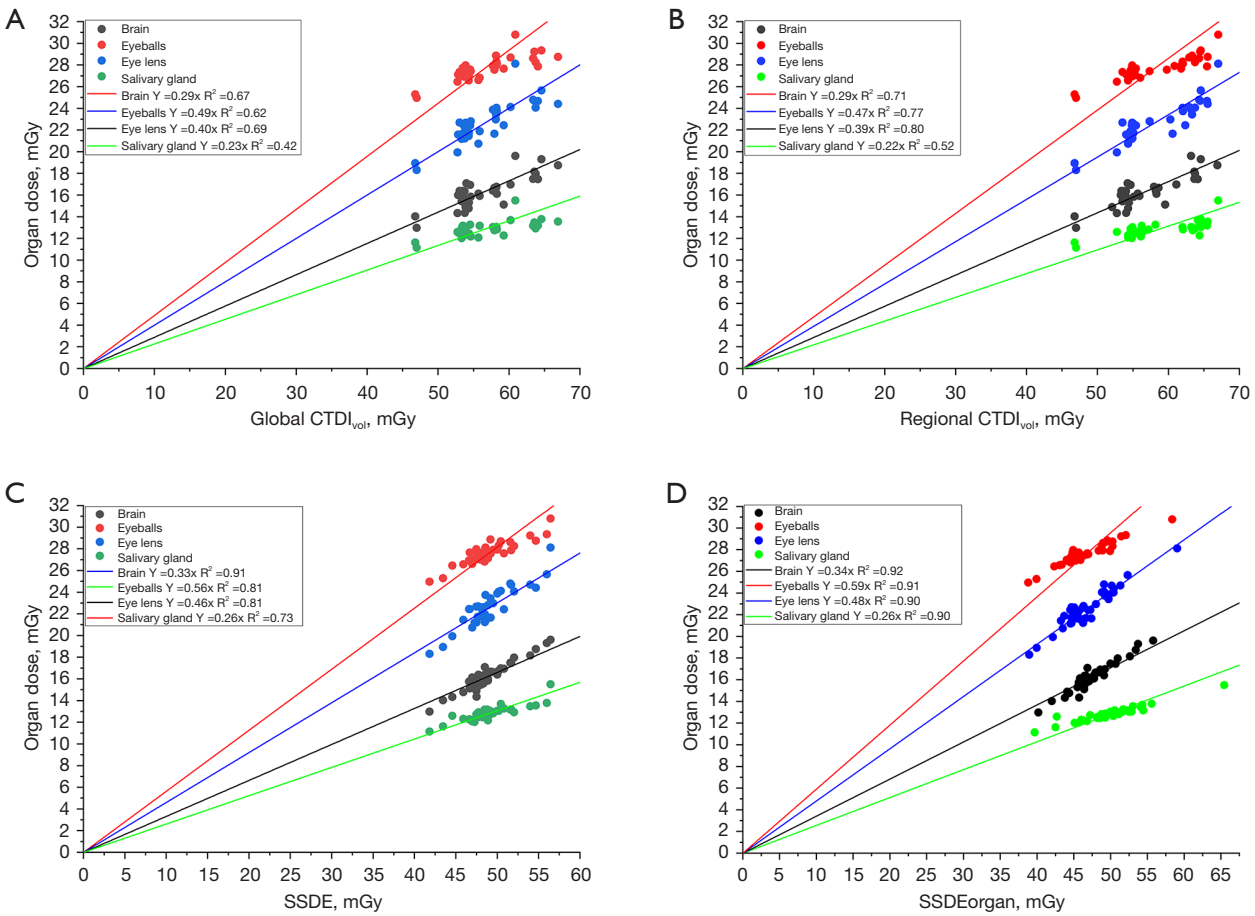

Figure 4 Results of linear regression fitting between each organ dose and each radiation dose metric in ODM head exams for (A) global $CTDI_{vol}$, (B) regional $CTDI_{vol}$, (C) SSDE, and (D) organ-specific SSDE. CT, computed tomography; $CTDI_{vol}$, volume CT dose index; ODM, organ dose modulation; SSDE, size-specific dose estimate.

the same methods as the papers of Huang and Papadakis *et al.* (8,25). The results in *Table 1* show that the maximum discrepancy between the 100° and 260° models and the 360° calculations was just 0.05% for different scanning protocols. This result validated the feasibility of scanning a 360° source model by splitting it into two parts. Based on *Table 3*, the $CTDI_w$ values calculated using MC simulation agreed with the experimental measurements, with an error rate of less than 5%. This confirms that splitting the model into two parts based on the angular range has minimal impact on particle motion and deposition.

Compared with $CTDI_{vol}$, SSDE is more effective in reflecting the absorbed dose of the patients. However, the value can only represent the individualized radiation dose related to the patient's body size with uniform tissue attenuation. Although the organ dose calculated using MC simulation is more accurate than other methods, this method is time-consuming and laborious and cannot be widely used in clinical practice. Therefore, our study evaluated the correlation between organ doses calculated using MC simulation and other metrics, including global $CTDI_{vol}$, organ-based regional $CTDI_{vol}$, SSDE, and organ-specific SSDE for the brain, eyeballs, lens, and salivary glands. Based on *Figure 4*, it was found that the R^2 between organ doses and their respective organ-based regional $CTDI_{vol}$, SSDE, and organ-specific SSDE was significantly higher than that of global $CTDI_{vol}$, except for the brain, where the R^2 between organ doses and global $CTDI_{vol}$ and organ-based regional $CTDI_{vol}$ was not significant. This may be attributed to the fact that the brain covers almost the entire scanning area in head CT examinations, and therefore, the difference between brain-based regional $CTDI_{vol}$ and global $CTDI_{vol}$ is minimal. The organ dose displayed a much stronger linear relationship with the organ-specific SSDE than other dose metrics, with R^2 values of 0.92, 0.90, 0.90, and 0.90 for each respective organ. This trend is consistent with the findings of Fujii *et al.* (16,26). The main reason for this phenomenon is that, compared to the global $CTDI_{vol}$, which only indicates the output radiation of the CT machine, the organ-based regional $CTDI_{vol}$ takes into account the tube current variation with the X-ray attenuation characteristics at each organ's Z-axis position. Meanwhile, SSDE considers both the patient's body size variations and tissue attenuation characteristics, and the organ-specific SSDE considers all of these factors simultaneously. Therefore, regression fitting using the organ-specific SSDE offers a more precise estimate of the organ dose than other metrics such as global $CTDI_{vol}$, organ-based regional $CTDI_{vol}$, and SSDE.

Figure 4 demonstrates that the estimation coefficients from SSDE to organ dose varied for different organs such as the brain, eyeballs, lens, and the salivary glands. Specifically, the estimation coefficients were 0.34, 0.59, 0.48 and 0.26, respectively. Garzón *et al.* analyzed the correlation of the SSDE with the organ dose for 139 head CT scans (11). The results showed that the organ dose of the brain and the eyes had a high correlation with SSDE (R^2=0.98, 0.97), consistent with our study's findings. However, the estimation coefficients for the organ doses ranged from 1.12 to 1.38 and from 1.13 to 1.28, respectively, which differed from the values obtained in our study. The disparities between this experiment and Garzón *et al.*'s study can be attributed to two main factors. Firstly, the patients in this experiment were exclusively adults, whereas Garzón *et al.*'s study focused on pediatric patients aged 0–15 years. Secondly, Garzón's study gathered data from 139 patients, employing the fixed tube current technique. At the same time, our study utilized the ODM technique in all cases. This also indicates that the CF used in prior research to estimate organ doses for head CT scans based on fixed or Z-axis tube current modulation cannot be applied to the ODM technique.

Studies have shown a strong correlation between organ dose and WED, which characterizes the individual body parameters (13,27). In addition to the method of estimating the organ dose of the examinee using CT dose metrics, the MC simulation method was used by Tahiri *et al.* to explore the feasibility of estimating the organ dose of head CT examination based on WED (13). Their findings indicated that after normalizing the organ doses using $CTDI_{vol}$, the correlation between each organ dose and WED was highly positively correlated for the brain (R^2>0.92), eyes (R^2>0.88), and lens (R^2>0.89). Regarding the R^2 of patient organ dose and organ-specific SSDE, our results are in high agreement with those of Tahiri *et al.* McMillan *et al.* conducted a study revealing that the dose of the brain and lens are more closely related to a patient's size in both spiral and axial head CT examinations. This means that organ doses can be predicted for the same CT scanner by considering the patient's body size and $CTDI_{vol}$ (27). In addition, Chen *et al.* investigated the effects of age and head circumference on SSDE, and the results showed that head circumference was significantly negatively correlated with SSDE in the younger patient group, but this trend was not observed in the older patient group, suggesting that the relationship between head circumference and SSDE is complex and not

simply linear, and that there is a relationship between the estimation of SSDE and age (28). This approach simplifies the calculation process and improves work efficiency, making it worthwhile to explore further.

There were certain limitations to this study. Firstly, the CT source model was based on a simplified version of the bowtie filter, which may not accurately represent its actual shape. As a result, some things could be improved in the simulation calculation of organ dose. For example, our source modeling method is based on the cookie-cutter technique, which does not take into account the actual focus size. In recent years, researchers have constructed fan-beam source modeling based on the actual CT tube, which has greatly improved the reliability; and the modeling accuracy of the bowtie filter also needs to be improved. Additionally, it is essential to note that the findings of this study are specific to Revolution CT scanners manufactured by GE; thus, they are not applicable to other manufacturers who use different ODM technologies with varying working principles. More precise modeling methods will be employed to construct the bowtie filter, and various vendors' angular modulation models will be used to accurately calculate the organ dose of CT scan.

Conclusions

In this study, in a head CT examination with angular modulation, we investigated the correlation between organ dose and different dose metrics (e.g., global $CTDI_{vol}$, organ-based regional $CTDI_{vol}$, SSDE, and organ-specific SSDE) for four specific organs, namely, the brain, eyeballs, lens, and salivary glands. Using linear regression fitting, we found that the correlation between organ dose and organ-specific SSDE demonstrated superior robustness compared to other dose metrics. As a result, a linear regression utilizing organ-specific SSDE could be a reliable and straightforward method for accurately estimating organ dose for patients undergoing head CT examination with ODM technology.

Acknowledgments

None.

Footnote

Reporting Checklist: The authors have completed the STROBE reporting checklist. Available at https://qims.amegroups.com/article/view/10.21037/qims-24-2061/rc

Funding: This work was supported by the Key Natural Science Project of Anhui Provincial Education Department (grant No. KJ2021A0746).

Conflicts of Interest: All authors have completed the ICMJE uniform disclosure form (available at https://qims.amegroups.com/article/view/10.21037/qims-24-2061/coif). The authors have no conflicts of interest to declare.

Ethical Statement: The authors are accountable for all aspects of the work in ensuring that questions related to the accuracy or integrity of any part of the work are appropriately investigated and resolved. This study was performed with the approval of Bengbu Medical University Ethics Committee (No. 2021-292) and was conducted following the guidelines of the Declaration of Helsinki (as revised in 2013). The Ethics Committee waived the need for informed consent for this retrospective study.

References

1. Yabuuchi H, Kamitani T, Sagiyama K, Yamasaki Y, Matsuura Y, Hino T, Tsutsui S, Kondo M, Shirasaka T, Honda H. Clinical application of radiation dose reduction for head and neck CT. Eur J Radiol 2018;107:209-15.
2. Omer H, Alameen S, Mahmoud WE, Sulieman A, Nasir O, Abolaban F. Eye lens and thyroid gland radiation exposure for patients undergoing brain computed tomography examination. Saudi J Biol Sci 2021;28:342-6.
3. Poon R, Badawy MK. Radiation dose and risk to the lens of the eye during CT examinations of the brain. J Med Imaging Radiat Oncol 2019;63:786-94.
4. Sheppard JP, Nguyen T, Alkhalid Y, Beckett JS, Salamon N, Yang I. Risk of Brain Tumor Induction from Pediatric Head CT Procedures: A Systematic Literature Review. Brain Tumor Res Treat 2018;6:1-7.
5. Hauptmann M, Byrnes G, Cardis E, Bernier MO, Blettner M, Dabin J, et al. Brain cancer after radiation exposure

from CT examinations of children and young adults: results from the EPI-CT cohort study. Lancet Oncol 2023;24:45-53.
6. Kosaka H, Monzen H, Amano M, Tamura M, Hattori S, Kono Y, Nishimura Y. Radiation dose reduction to the eye lens in head CT using tungsten functional paper and organ-based tube current modulation. Eur J Radiol 2020;124:108814.
7. Kitera N, Matsubara K, Fujioka C, et al. Organ-based Tube-current Modulation Applied on Different MDCT Scanners: Reduction in the Radiation Dose to the Eye Lens at Head CT. Nihon Hoshasen Gijutsu Gakkai Zasshi 2020;76:366-74.
8. Huang Y, Zhuo W, Gao Y, Liu H. Monte Carlo simulation of eye lens dose reduction from CT scan using organ based tube current modulation. Phys Med 2018;48:72-5.
9. Damilakis J. CT Dosimetry: What Has Been Achieved and What Remains to Be Done. Invest Radiol 2021;56:62-8.
10. Shao W, Lin X, Huang Y, Qu L, Zhuo W, Liu H. Rapid patient-specific organ dose estimation in computed tomography scans via integration of radiomics features and neural networks. Quant Imaging Med Surg 2024;14:7379-91.
11. Garzón WJ, Aldana DFA, Cassola VF. PATIENT-SPECIFIC ORGAN DOSES FROM PEDIATRIC HEAD CT EXAMINATIONS. Radiat Prot Dosimetry 2020;191:1-8.
12. Moore BM, Brady SL, Mirro AE, Kaufman RA. Size-specific dose estimate (SSDE) provides a simple method to calculate organ dose for pediatric CT examinations. Med Phys 2014;41:071917.
13. Tahiri M, Benameur Y, Mkimel M, El Baydaoui R, Mesardi MR. Feasibility of size-specific organ-dose estimates based on water equivalent diameter for common head CT examinations: a Monte Carlo study. J Radiol Prot 2023;43:021503.
14. Hardy AJ, Bostani M, Kim GHJ, Cagnon CH, Zankl MA, McNitt-Gray M. Evaluating Size-Specific Dose Estimate (SSDE) as an estimate of organ doses from routine CT exams derived from Monte Carlo simulations. Med Phys 2021;48:6160-73.
15. Bostani M, McMillan K, Lu P, Kim GH, Cody D, Arbique G, Greenberg SB, DeMarco JJ, Cagnon CH, McNitt-Gray MF. Estimating organ doses from tube current modulated CT examinations using a generalized linear model. Med Phys 2017;44:1500-13.
16. Fujii K, Nomura K, Muramatsu Y, Goto T, Obara S, Ota H, Tsukagoshi S. Correlation analysis of organ doses determined by Monte Carlo simulation with dose metrics for patients undergoing chest-abdomen-pelvis CT examinations. Phys Med 2020;77:1-9.
17. Turner AC, Zhang D, Kim HJ, DeMarco JJ, Cagnon CH, Angel E, Cody DD, Stevens DM, Primak AN, McCollough CH, McNitt-Gray MF. A method to generate equivalent energy spectra and filtration models based on measurement for multidetector CT Monte Carlo dosimetry simulations. Med Phys 2009;36:2154-64.
18. Punnoose J, Xu J, Sisniega A, Zbijewski W, Siewerdsen JH. Technical Note: spektr 3.0-A computational tool for x-ray spectrum modeling and analysis. Med Phys 2016;43:4711.
19. Gu J, Bednarz B, Caracappa PF, Xu XG. The development, validation and application of a multi-detector CT (MDCT) scanner model for assessing organ doses to the pregnant patient and the fetus using Monte Carlo simulations. Phys Med Biol 2009;54:2699-717.
20. Pan Y, Qiu R, Gao L, Ge C, Zheng J, Xie W, Li J. Development of 1-year-old computational phantom and calculation of organ doses during CT scans using Monte Carlo simulation. Phys Med Biol 2014;59:5243-60.
21. DeMarco JJ, Cagnon CH, Cody DD, Stevens DM, McCollough CH, O'Daniel J, McNitt-Gray MF. A Monte Carlo based method to estimate radiation dose from multidetector CT (MDCT): cylindrical and anthropomorphic phantoms. Phys Med Biol 2005;50:3989-4004.
22. Khatonabadi M, Kim HJ, Lu P, McMillan KL, Cagnon CH, DeMarco JJ, McNitt-Gray MF. The feasibility of a regional CTDIvol to estimate organ dose from tube current modulated CT exams. Med Phys 2013;40:051903.
23. Burton CS, Szczykutowicz TP. Evaluation of AAPM Reports 204 and 220: Estimation of effective diameter, water-equivalent diameter, and ellipticity ratios for chest, abdomen, pelvis, and head CT scans. J Appl Clin Med Phys 2018;19:228-38.
24. Hardy AJ, Bostani M, Hernandez AM, Zankl M, McCollough C, Cagnon C, Boone JM, McNitt-Gray M. Estimating a size-specific dose for helical head CT examinations using Monte Carlo simulation methods. Med Phys 2019;46:902-12.
25. Papadakis AE, Damilakis J. Evaluation of an organ-based tube current modulation tool in pediatric CT examinations. Eur Radiol 2020;30:5728-37.
26. Fujii K, Nomura K, Muramatsu Y, Ota H. Patient-specific organ dose evaluation based on Monte Carlo simulation and dose metrics in paediatric chest-abdomen-pelvis CT examinations. Radiat Prot Dosimetry 2021;197:46-53.

27. McMillan K, Bostani M, Cagnon C, Zankl M, Sepahdari AR, McNitt-Gray M. Size-specific, scanner-independent organ dose estimates in contiguous axial and helical head CT examinations. Med Phys 2014;41:121909.
28. Chen T, Kong X, Peng W, Liao T, Hu H, Pan N, Yuan Z. Applying the AAPM 293 report to estimate the absorbed dose during head computed tomography: using head circumference for rapid dose estimation. Quant Imaging Med Surg 2023;13:3140-9.

Cite this article as: Wang M, Qin T, Fan Y, Xie Z, Liang B. Correlation analysis of organ doses with dose metrics for patients undergoing organ dose-modulated head CT examinations. Quant Imaging Med Surg 2025;15(5):3849-3860. doi: 10.21037/qims-24-2061